JOURNAL OF SPACECRAFT AND ROCKETS
Vol. 43, No. 6, November–December 2006

Engineering Notes

ENGINEERING NOTES are short manuscripts describing new developments or important results of a preliminary nature. These Notes should not exceed 2500 words (where a figure or table counts as 200 words). Following informal review by the Editors, they may be published within a few months of the date of receipt. Style requirements are the same as for regular contributions (see inside back cover).

Effects of Angle-of-Attack on the Aeroelastic Characteristics of a Wing with Freeplay

Young-Keun Park,* Jae-Han Yoo,† and In Lee‡
Korea Advanced Institute of Science and Technology, Daejeon 305-701, Republic of Korea
and
Dae-Yeal Lee§
Agency for Defense Development, Daejeon 305-600, Republic of Korea

DOI: 10.2514/1.21368

I. Introduction

A great deal of interest for the nonlinear aeroelastic approach of lifting surfaces has been manifested in the last decade or so. Within such an approach, both the aerodynamic and structural nonlinearities have to be incorporated in the related aeroelastic governing equations. Among the structural nonlinearities, the freeplay is inevitable for control surfaces of flight vehicles due to normal wear of components and manufacturing mismatches. In addition, the aerodynamic nonlinearities induced by the shock waves in the transonic region should be included. As is well known, the latter nonlinearities exert a deleterious effect on the limit cycle oscillation (LCO) and on transonic dip. Furthermore, for evident reasons, the air vehicle flies at an angle-of-attack that can affect the flutter characteristics in the transonic flight speed range.

Some aeroelastic analyses with freeplay have been performed in the past. Bae et al. [1] investigated the nonlinear aeroelastic characteristics of a wing with freeplay using frequency and time domain analysis methods. For aerodynamic nonlinearity, Kim and Lee [2] and Kwon et al. [3] performed an aerodynamic analysis of a wing in the transonic region using the transonic small disturbance (TSD) code, which was also applied in this study. These results were directly compared to the wind-tunnel experiments of the NLR [4] in transonic and supersonic flow regions, and they agreed well with the experimental steady and unsteady pressure distributions of the F-5 wing model. Yoo et al. [5] presented an efficient nonlinear aeroelastic analysis method that can deal with aerodynamic nonlinearity due to transonic shock wave and structure nonlinearity due to freeplay. In the study, the developed method, which was also applied in this study, was verified, and nonlinear aeroelastic responses in the transonic region were compared to those in a subsonic region. Yoo et al. [6] investigated the effects of the initial angle-of-attack on the aeroelastic characteristics in the transonic and supersonic regions by using the TSD aerodynamic theory. In the transonic region, there were large changes of aerodynamic characteristics due to the effect of static deformation with an initial angle-of-attack. Kholodar and Dowell [7] carried out studies on the angle-of-attack effects of a three-degree-of-freedom airfoil model with freeplay in the flap rotation. A vortex lattice aerodynamic model and a reduced-order aerodynamic technique were used to calculate unsteady aerodynamic forces in a low subsonic region. The LCO and chaotic motion occurred over a wide range of velocities for small angles of attack, and the responses converged to a static equilibrium state as the angle-of-attack increased.

In this study, a 3-D all-movable control wing with freeplay was used to show how the aeroelastic response characteristics vary with the initial angle-of-attack and the Mach number in subsonic and transonic regions. The fictitious mass (FM) method is used to apply a modal approach to nonlinear structural models. The TSD equation is used to calculate unsteady aerodynamic forces in the transonic region. Nonlinear aeroelastic time responses are computed by the coupled time integration method (CTIM).

II. Nonlinear Aeroelastic Equations and Numerical Methods

The motion equation of an aeroelastic system with structural nonlinearities can be written as

$$[M]\{\ddot{u}\} + [C]\{\dot{u}\} + \{R(u)\} = \{F(t, u, \dot{u})\} \tag{1}$$

where $[M]$ and $[C]$ are the mass and damping matrices, $\{u\}$ and $\{F\}$ are the displacement and external aerodynamic force vectors, respectively, and $\{R(u)\}$ is the elastic restoring force vector, including structural nonlinearities. The structural nonlinear elastic restore force vector $\{R(u)\}$ can be written as

$$\{R(u)\} = [K]\{u\} + \{f(\alpha)\} \tag{2}$$

where $[K]$ is the linear stiffness matrix and $\{f(\alpha)\}$ is the restoring force vector due to structural nonlinear factors and is given as

$$f(\alpha) = \begin{cases} K_\alpha(\alpha - s) & ,\alpha > s \\ 0 & ,-s \le \alpha \le s \\ K_\alpha(\alpha + s) & ,\alpha < -s \end{cases} \tag{3}$$

where K_α, α, and s are linear stiffness, pitch angle, and freeplay angle, respectively, at the freeplay node.

Usually, the aeroelastic analysis is conducted by using a mode approach method with a limited number of low-frequency modes to reduce the computational effort required. For air vehicle wings with freeplay, the normal mode approach cannot be used due to the stiffness variation with the displacement. Karpel and Wieseman [8] propose the FM method to overcome this difficulty. Lee and Kim [9] describe the application of the FM method to a 3-D wing with freeplay. After the modal matrix, $[\phi_b]$, is obtained from the FM model, the displacement vector can be expressed as

Received 25 November 2005; revision received 12 April 2006; accepted for publication 24 April 2006.

*Graduate Research Assistant, Division of Aerospace Engineering, 373-1 Guseong-Dong, Yuseong-gu; currently with Agency for Defense Development.

†Graduate Research Assistant, Division of Aerospace Engineering, 373-1 Guseong-Dong, Yuseong-gu.

‡Professor, Division of Aerospace Engineering, 373-1 Guseong-Dong, Yuseong-gu, Associate Fellow AIAA.

§Principal Researcher, Yuseong P.O.BOX 35-3.

$$\{u(t)\} = [\phi_b]\{q(t)\} \tag{4}$$

where $\{q\}$ is the generalized displacement vector. Transformation of Eq. (1) into the modal coordinate system gives

$$[\mathrm{GM}]\{\ddot{q}\} + [\mathrm{GC}]\{\dot{q}\} + \{\mathrm{GR}(u)\} = \{Q(t, q, \dot{q})\} \tag{5}$$

where [GM] and [GC] are the generalized mass and damping matrices, respectively. Furthermore, [GR] is the generalized restoring force vector defined as $[\phi_b]^T[K][\phi_b]\{q\} - [\phi_b]^T\{f(\alpha)\}$ and $\{Q\}$ is the generalized external aerodynamic force vector and can be obtained from summation of pressure distribution on wing surfaces, which is obtained from the TSD equation. The theoretical background and verification of the applied method in this study are described in detail in [5].

III. Results and Discussion

As a computational example, an all-movable control wing model with freeplay around its hinge axis is considered in this study, as shown in Fig. 1. The wing model has a root chord of 0.156 m, an aspect ratio of 2.564, a taper ratio of 0.5, and a sweptback angle of 27.47 deg. The structural thickness of the wing is 2 mm, the linear stiffness, K_α, is 100 N · m/rad, and the freeplay angle s is 0.1 deg. For the wing section, 4% biconvex airfoil is used.

Figure 2a shows the chordwise differential (lower surface minus upper) pressure coefficient distributions at the midspan for the Mach numbers 0.5, 0.85, 0.9, and 0.95, for a model with an initial angle-of-attack of 2 deg before the wing has been deformed by an angle-of-attack. The differential pressure distribution changes slightly as the Mach number increases in the subsonic region. At $M = 0.9$, a weak shock appears on the upper and lower surfaces of control wing with a 0 deg angle-of-attack, whereas with an angle-of-attack, the lower surface shock disappears while the upper surface shock moves to the trailing edge. At $M = 0.95$, the pressure distribution has a shock doublet at the mean (0 deg angle-of-attack) shock location, $x/c = 0.93$. The width of the shock doublet is indicated by the vertical lines: the forward one is at the lower surface shock location and the rear one is at the upper surface location. These differential pressure distributions accordingly produce a pitching moment around the hinge axis and an angular displacement. Dowell and Ilgamov [10] showed similar results for NACA 64A006 airfoil.

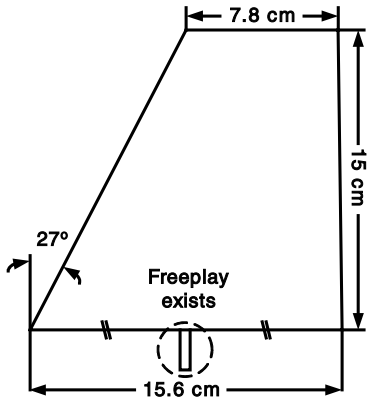

a)

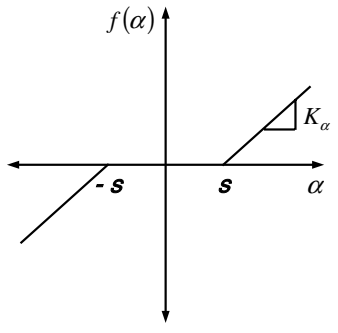

b)

Fig. 1 a) Geometric configuration of the control wing model. b) Restoring moment for pitch angle α with a symmetric freeplay.

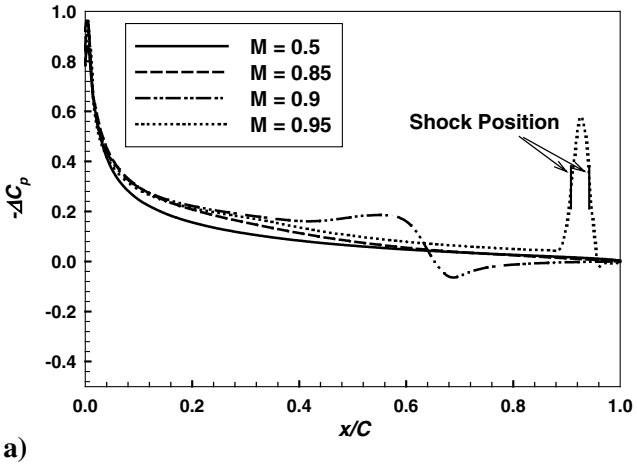

a)

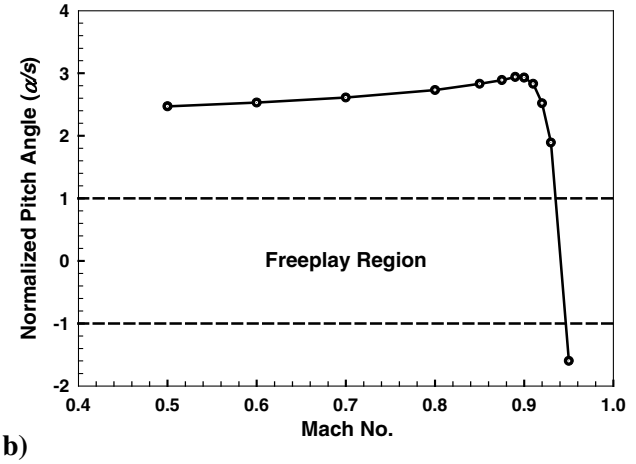

b)

Fig. 2 a) Distributions of steady pressure coefficient differences at midspan station of undeformed wing. b) Normalized pitch angle vs Mach number of the deformed wing.

Figure 2b shows the normalized angular displacement against a Mach number at the same dynamic pressure. Angular displacement was then defined as angles around the hinge axis in a static equilibrium state after the wing has been deformed by an angle-of-attack. This means that the control wing is preloaded around the hinge axis because of the pitching moment by the angle-of-attack. For a Mach number between 0.5 and 0.85, where shock waves do not occur, the angular displacement increases gradually with the Mach number. That means the pitching moment increases with the Mach number in a subsonic region. From Mach number 0.9, where a weak shock occurs on the upper surface, the shock doublet moves toward the trailing edge as the Mach number increases. As a result, the pitching moment decreases and so does angular displacement. At around Mach 0.94 the pitching moment decreases to zero and becomes negative at Mach 0.95 so that the control wing deforms nosedown about the pitch axis. This pitching moment has a close relationship with the variations of aeroelastic characteristics with freeplay.

Figure 3 shows the normalized pitch angle responses against the velocity for the control wing with freeplay at various Mach numbers in cases in which the angles of attack are 0 and 2 deg. Here, the initial disturbance is given by the pitch angle, $\alpha_0 = 1.6$ deg, defined as the angular displacement about the hinge axis with the rigid body

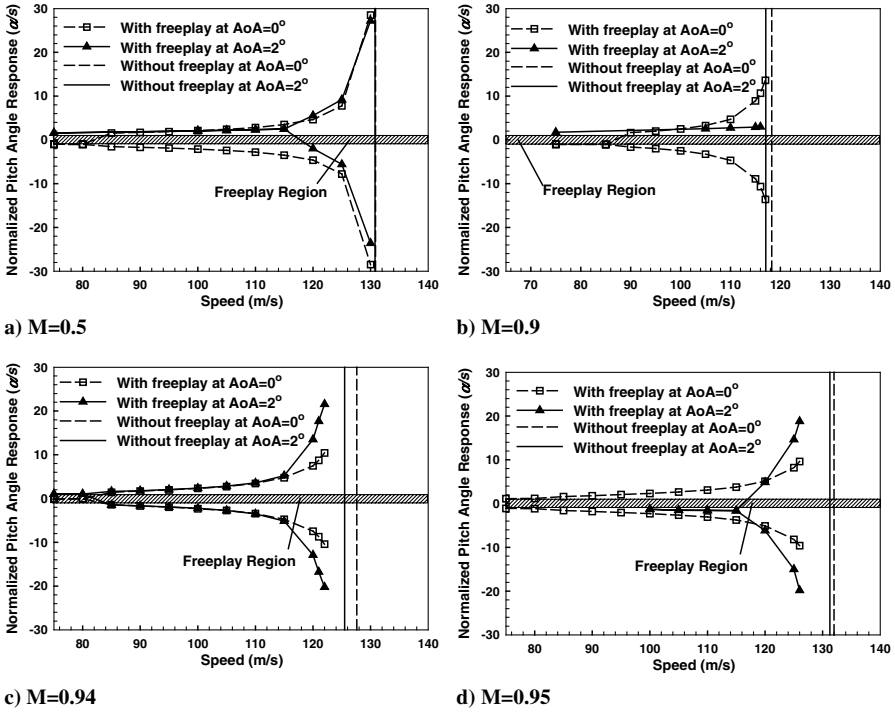

Fig. 3 Normalized pitch angle response vs Mach number of the control wing model.

rotation of the wing. The pitch angle response means the maximum/minimum value of α when $\dot{\alpha} = 0$. If at a particular velocity the oscillation is damped out to a static equilibrium state, then a single point response is obtained, and if the motion is an LCO, then two points are obtained.

Figure 3a shows the aeroelastic analysis results at Mach 0.5. The flutter velocity without freeplay is 130.8 m/s at Mach 0.5, and its variation is negligible with the angle-of-attack. As might be expected, the LCO occurs below the flutter velocity with freeplay. For a 0 deg angle-of-attack, the pitch oscillation is damped out to a static equilibrium state below $V = 80$ m/s. The static equilibrium state is slightly off the neutral axis by the freeplay, although the cross section of wing is symmetric. As the velocity increases past that value, the LCO responses begin to appear, and its amplitudes increase exponentially and diverge near the flutter velocity. For a 2 deg angle-of-attack, the pitch oscillation is damped out to a static equilibrium state below $V = 115$ m/s, and the LCO begins to occur at $V = 115$–120 m/s. LCO onset velocity increases greatly compared to a 0 deg angle-of-attack. These LCO characteristics with the initial angle-of-attack have a close relationship with the size of the preload. The preload of the hinge axis reduces the effect of freeplay so that the LCO onset velocity increases.

Figure 3b shows the aeroelastic analysis results at Mach 0.9. As explained before, at Mach 0.9 shock appears and a large preload pitching moment occurs due to the initial angle-of-attack. The flutter velocities without freeplay are 118.3 and 117.1 m/s for 0 and 2 deg angles of attack, respectively. Note that at Mach 0.9 the flutter velocity deceases with the angle-of-attack, but this decrease was negligible at $M = 0.5$. For a 0 deg angle-of-attack, the pitch oscillation is damped out to a static equilibrium state below $V = 85$ m/s and the LCO begins to occur at $V = 85$–90 m/s. For a 2 deg angle-of-attack, however, the pitch oscillation is damped out just below flutter velocity without the LCO and then diverges near the flutter velocity. At Mach 0.9, the preloaded pitching moment caused by the angle-of-attack increases compared to that at Mach 0.5, so the freeplay effects decrease and LCO disappears.

Figure 3c shows the aeroelastic analysis results at Mach 0.94. The flutter velocities without freeplay are 127.6 and 125.5 m/s for 0 and 2 deg angles of attack, respectively, at Mach 0.94. The flutter velocity decreases a bit with the angle-of-attack, as in the cases of Mach 0.9. For the model with freeplay, the pitch oscillation is damped out to a static equilibrium state below $V = 80$ m/s, and the LCO begins to occur at $V = 80$–85 m/s and diverges at around $V = 123$ m/s, which is below the flutter velocity at 0 and 2 deg angles of attack. The angle-of-attack is shown to have little effect on the LCO characteristics compared to Mach 0.5 and 0.9, and this is due to the considerable effect of freeplay, in which the pitching moment is close to zero for a 2 deg angle-of-attack, as it is for a 0 deg angle-of-attack.

Figure 3d represents the aeroelastic analysis results at Mach 0.95. The flutter velocities without freeplay are 132.0 and 131.4 m/s for 0 and 2 deg angles of attack, respectively. The flutter velocity decreases a bit with the angle-of-attack as in the cases of Mach 0.9 and 0.94. The pitch displacement does not converge to a static equilibrium state below $V = 80$ m/s at a 0 deg angle-of-attack and keeps oscillating in a low frequency with a similar amplitude to the freeplay size. The LCO occurs at $V = 80$–85 m/s and diverges at around $V = 127$ m/s, which is below the flutter velocity. The pitch displacement converges to a static equilibrium state below $V = 115$ m/s at a 2 deg angle-of-attack, and the direction of the control wing deflection is nosedown unlike at Mach 0.5 and 0.9. The LCO onset velocity is much higher for a 2 deg angle-of-attack than for one of 0 deg. This tendency was similar at Mach 0.5.

IV. Conclusions

In this study, aeroelastic analyses were conducted for the control wing model with freeplay and an initial angle-of-attack in subsonic and transonic flow regions. For the wing model without freeplay, the initial angle-of-attack caused a slight decrease in flutter stability in the transonic region. When the wing had the freeplay, the LCO started at a very low speed in the transonic region as well as the subsonic region. The present results showed that the initial angle-of-attack could increase the onset speed of the LCO in the subsonic and the most of the transonic flow regions. However, there was a certain Mach number in which the effects of the initial angle-of-attack were negligible, because the pitching moment on the wing was close to zero for that Mach number.

Acknowledgment

Authors are gratefully acknowledging the support by Agency for Defense Development and by Flight Vehicle Research Center (FVRC), Seoul National University.

References

[1] Bae, J. S., Yang, S. M., and Lee, I., "Linear and Nonlinear Aeroelastic Analysis of a Fighter-Type Wing with Control Surface," *Journal of Aircraft*, Vol. 39, No. 4, 2002, pp. 697–708.

[2] Kim, D. H., and Lee, I., "Transonic and Low-Supersonic Aerodynamic Analysis of a Wing with Underpylon/Store," *Journal of Aircraft*, Vol. 37, No. 1, 2000, pp. 189–192.

[3] Kwon, H. J., Kim, D. H., and Lee, I., "Frequency and Time Domain Flutter Computations of a Wing with Oscillating Control Surface Including Shock Interference Effects," *Aerospace Science and Technology*, Vol. 8, No. 6, 2004, pp. 519–532.

[4] Tijdeman, H., van Nunen, J. W. G., Kraan, A. N., Persoon, A. J., Poestkoke, R., Schippers, P., and Siebert, C. M., "Transonic Wind Tunnel Tests on an Oscillating Wing with External Stores; Parts 1–4," National Aerospace Lab of The Netherlands, NLR-TR-78106, AFFDL-TR-78-194, 1978.

[5] Yoo, J. H., Park, Y. K., Lee, I., and Han, J. H., "Aeroelastic Analysis of a Wing with Freeplay in the Subsonic/Transonic Region," *JSME International Journal, Series B (Fluids and Thermal Engineering)*, Vol. 48, No. 2, 2004, pp. 208–211.

[6] Yoo, J. H., Kim, D. H., and Lee, I., "Angle-of-Attack Effect on the Transonic/Supersonic Aeroelasticity of Wing-Box Model," *Journal of Aircraft*, Vol. 39, No. 5, 2002, pp. 906–908.

[7] Kholodar, D. B., and Dowell, E. H., "Behavior of Airfoil with Control Surface Freeplay for Nonzero Angle of Attack," *AIAA Journal*, Vol. 37, No. 5, 1999, pp. 651–653.

[8] Karpel, M., and Wieseman, C. D., "Modal Coordinates for Aeroelastic Analysis with Large Local Structural Variation," *Journal of Aircraft*, Vol. 31, No. 2, 1994, pp. 396–400.

[9] Lee, I., and Kim, S. H., "Aeroelastic Analysis of a Flexible Control Surface with Structural Nonlinearity," *Journal of Aircraft*, Vol. 32, No. 4, 1995, pp. 868–874.

[10] Dowell, E. H., and Ilgamov, M., *Studies in Nonlinear Aeroelasticity*, Springer–Verlag, Daejon, Republic of Korea, 1988, pp. 212–215.

M. Miller
Associate Editor